

# The Comparative Analysis of Two Typical Fluidic Thrust Vectoring Exhaust Nozzles on Aerodynamic Characteristics

Xin H. Zou, Qiang Wang

**Abstract**—The comparisons of two typical fluidic thrust vectoring exhaust nozzles including two-dimensional(2-D) nozzle and axisymmetric nozzle on aerodynamic characteristics was presented by numerical simulation. The results show: the thrust vector angles increased with the increasing secondary flow but decreased with the nozzle pressure ratio (NPR) increasing. With the same secondary flow and NPR, the thrust vector angles of 2-D nozzle were higher than the axisymmetric nozzle's. So with the lower NPR and more secondary weight flow, the much higher thrust vector angle was caused by 2-D fluidic nozzle. And with the higher NPR and less secondary weight flow, there was not much difference in angular dimension between two nozzles.

**Keywords**—Aerodynamic characteristics , fluidic nozzle , vector angle , thrust coefficient comparison.

## I. INTRODUCTION

FLUIDIC thrust vectoring with the shock vector control method which is widely studied [ 1-6 ]at the moment, requires forced, asymmetric fluidic injection of a secondary air stream into the supersonic, primary flow that develops in the divergent section of the nozzle at certain conditions.

As two-dimensional (2-D) nozzle and axisymmetric nozzle widely studied [1-3], under the same parameters of geometric and aerodynamic, the numerical simulation on the nozzle internal flow was made. Accordingly, the comparative analysis of different weight flow and NPR on the thrust vectoring influence was present.

## II. COMPUTATIONAL METHOD

### A. Calculation format and Turbulence modeling

Algorithm used in this finite volume method time advance, the control equation of the general curvilinear coordinates used strong conservative form of N-S equations. To improve convergence speed and solution precision, the discrete choice format, Implicit second order upwind scheme.

A 2-equation ( RNG )  $k-\epsilon$  model was used as the turbulence modeling , with standard wall function

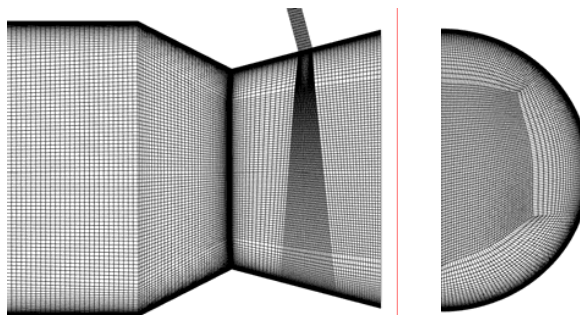
### B. Nozzle geometry

For the accurate qualitative analysis the geometric

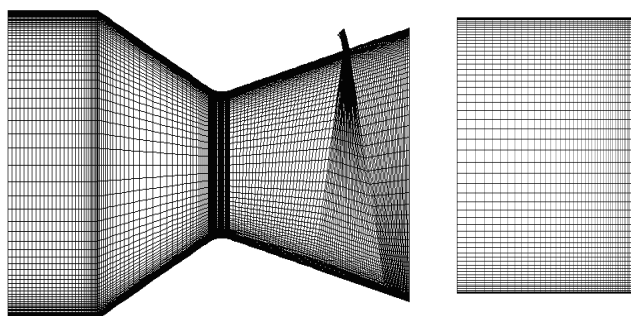
parameters of two nozzles were the same including the area of nozzle throat  $26\text{cm}^2$ , the area of primary nozzle inlet,  $56.66\text{cm}^2$ , the area of the nozzle outlet,  $50.4\text{cm}^2$ , the axial distance of the divergent section  $4.232\text{cm}$ , the area of the injection slot,  $2.065\text{cm}^2$ .

### C. Computational domain

The computational mesh was structured with local refinement Fig. 1 shows the symmetry plane grid of 2-D nozzle and axisymmetric nozzle.



(a). Symmetry plane of 2-D nozzle



(b). Symmetry plane of axisymmetric nozzle

Fig. 1 Computational mesh of two nozzles

Boundary conditions: The temperatures of primary and secondary flow were both  $300\text{k}$ . the NPR ranged from 4~10, the secondary weight flow ratio was 2.5%-10%. A first order extrapolation outflow condition was used at the downstream far field boundary. A no-slip adiabatic wall boundary condition was implemented to obtain viscous solutions.

X. H. Zou is with the School of Jet Propulsion, Beijing University of Aeronautics and Astronautics, Beijing, 100191 P.R. China (ses725@126.com)

Q. Wang is with the School of Jet Propulsion, Beijing University of Aeronautics and Astronautics, Beijing, 100191 P.R. China

### III. RESULTS AND DISCUSSION

#### A. Effect of secondary weight flow ratio on thrust vectoring

Fig.2 shows the vector angle comparison of two nozzles for the NPR=5. Generally, with the weight flow increasing, the vector angles all increased. The vector angles of the 2-D nozzle were higher than the axisymmetric nozzle's. under the same conditions., and the highest vector angle was 16°. Furthermore, there was not much difference with the less secondary weight flow (2.5%, 4%, 6%),but with the more secondary weight flow ( 8%, 10% ) the vector angle differed widely, and the largest angle difference was 5°when the secondary weight flow ratio was 10%.

Fig. 3 shows the thrust coefficient comparison of two nozzles for the NPR=5. Generally , the thrust coefficient were both increased with the more secondary weight flow . In addition, the thrust coefficient of the 2-D nozzle was higher than the axisymmetric nozzle's, and differed greatly with the less secondary weight flow. With the secondary weight flow ratio 10%, there was not much difference, which illustrated little effect on thrust coefficient with more secondary weight flow. Fig. 4 shows  $\omega=10\%$  the mach contours symmetry plane of two nozzles. Fig.4(b) and Fig.4(a), obviously, to the former, the recirculation region along the injection slot was larger than that along the later, and it made the pressure difference on the wall less which caused the vector angles excrescence. So under the same aerodynamic conditions, the vector angles of the axisymmetric nozzle were lower than the 2-D nozzle's.

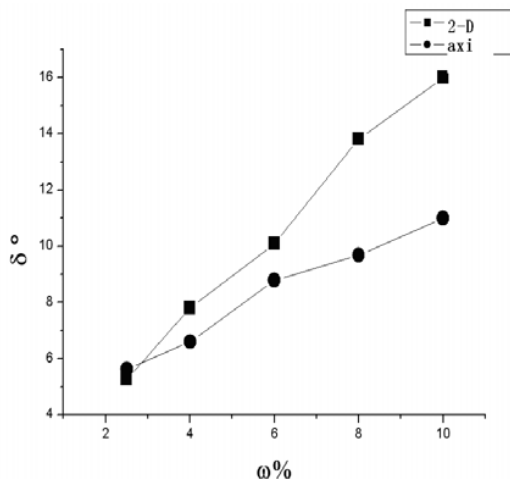


Fig. 2 The vector angle comparison with different secondary weight flow (NPR=5 )

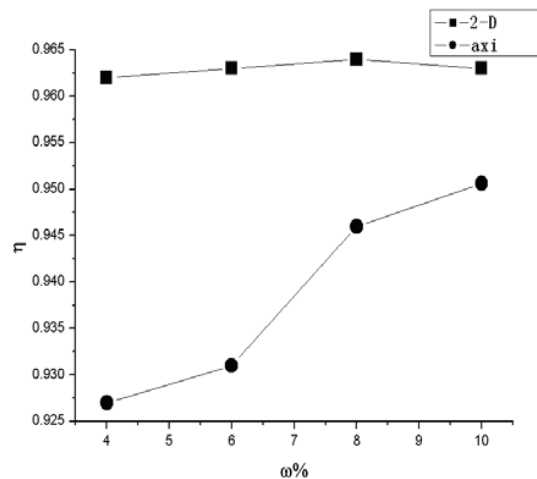
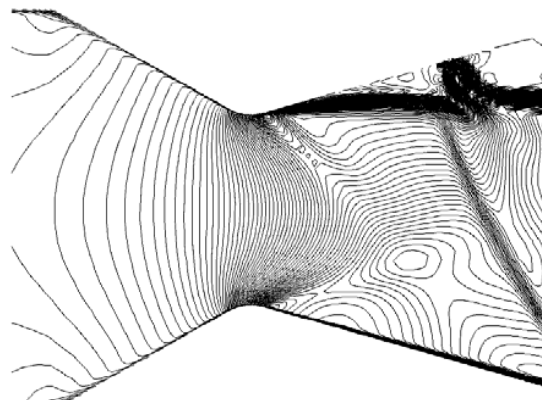
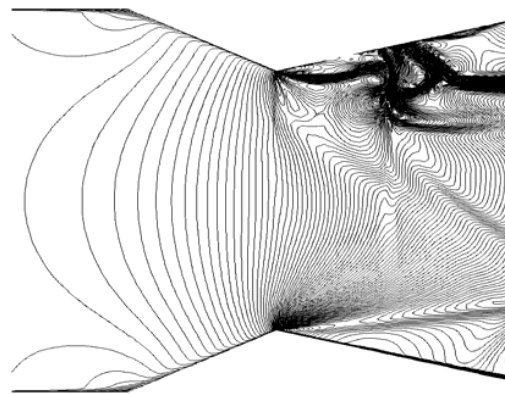


Fig. 3 The thrust coefficient comparison with different secondary weight flow ( NPR=5 )



(a). Symmetry plane of 2-D nozzle



(b). Symmetry plane of axisymmetric nozzle

Fig. 4 The mach contours of two nozzles symmetry plane (NPR=5ω=10%)

Fig.5 shows the vector angle comparison of two nozzles for

the NPR=7. The entire tendency was similar to Fig. 2. The highest thrust vector angle was  $12^\circ$ . Unlikely, the vector angle difference became less under the same secondary weight flow, especially was obvious as the  $\omega=4\%$ . As Fig. 6(a) shows the shock separation before the injection slot moved farther backward than that in Fig. 6(b), which caused not much difference in vector angles.

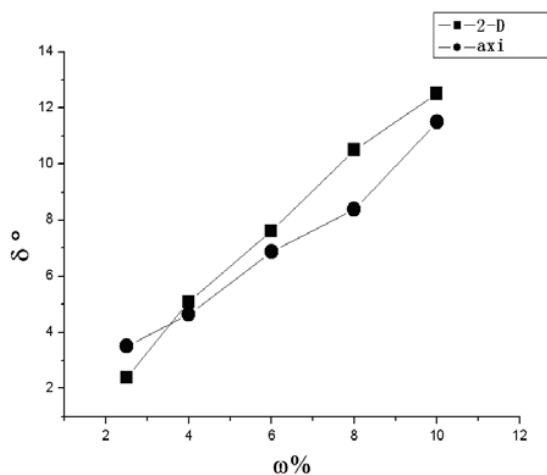
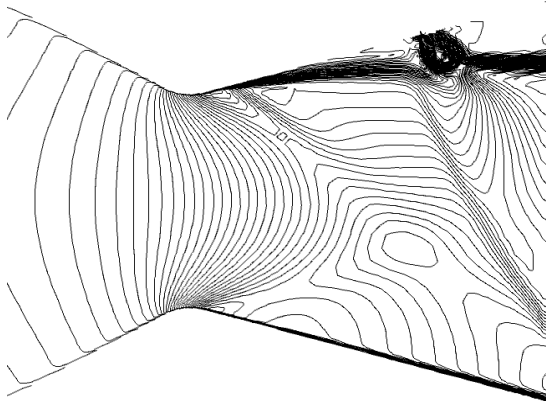
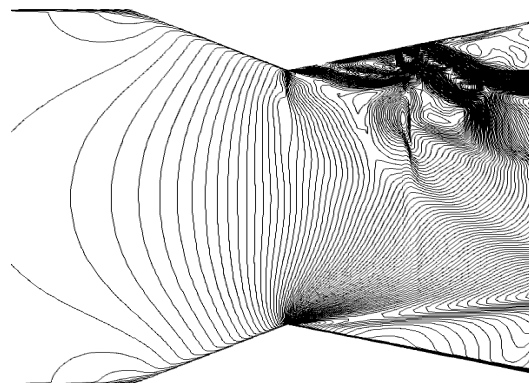


Fig. 5 The vector angle comparison with different secondary weight Flow ( NPR=7 )



(a). Symmetry plane of 2-D nozzle



(b). Symmetry plane of axisymmetric nozzle

Fig. 6 The mach contours of two nozzles symmetry plane (NPR=7,  $\omega=10\%$ )

Fig.7 shows the vector angle comparison of two nozzles for the NPR=10. The distribution of vector angles is similar to Fig. 5. The vector angles were all increased with the secondary weight flow increasing, and the highest angle was  $10.4^\circ$ . With the less secondary weight flow ( 2% , 4% ), there was not much difference in vector angles between two nozzles.

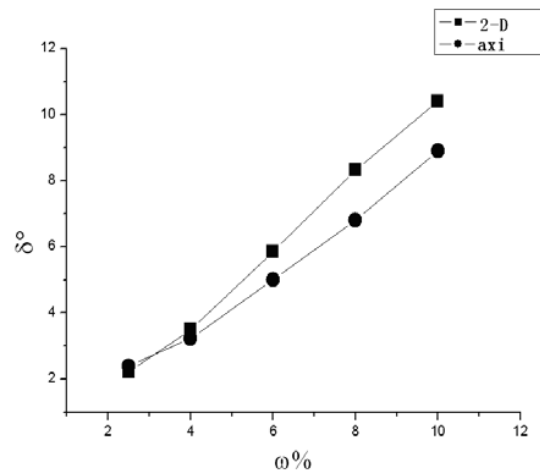


Fig. 7 The vector angle comparison with different secondary weight flow ( NPR=10 )

Figure8 shows the thrust coefficient comparison of two nozzles for the NPR=10. Unlike the lower NPR case (NRR=5), the thrust coefficient decreased with the secondary weight flow increasing.

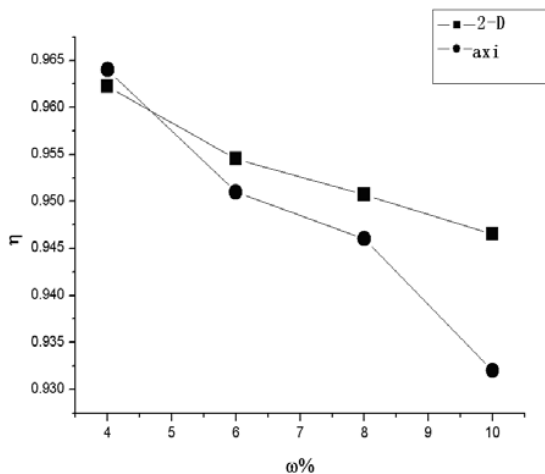
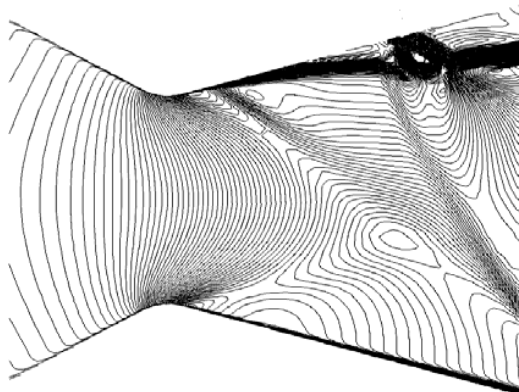
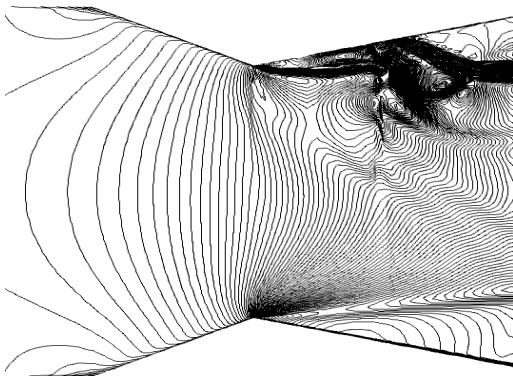


Fig. 8 The thrust coefficient comparison with different secondary weight flow (NPR=10)



(a). Symmetry plane of 2-D nozzle



(b). Symmetry plane of axisymmetric nozzle

Fig. 9 The mach contours of two nozzles symmetry plane (NPR=10  $\omega$  =10%)

#### B. Effect of the NPR on thrust vectoring

Fig.10 shows the vector angle comparison of two nozzles under different NPR for the  $\omega=4\%$ . On the whole, the vector angle of 2-D nozzle was higher than the axisymmetric nozzle's with the same reason as the conditions above. Moreover, the vector angles decreased with the NPR increasing. As seen in Fig.12, the pressure of downstream separation along the injection slot was equal to ambient pressure, so with the ambient and nearby wall pressure decreasing, the wall pressure difference decreased. It caused the vector angle lower and there was not much difference under the higher NPR.

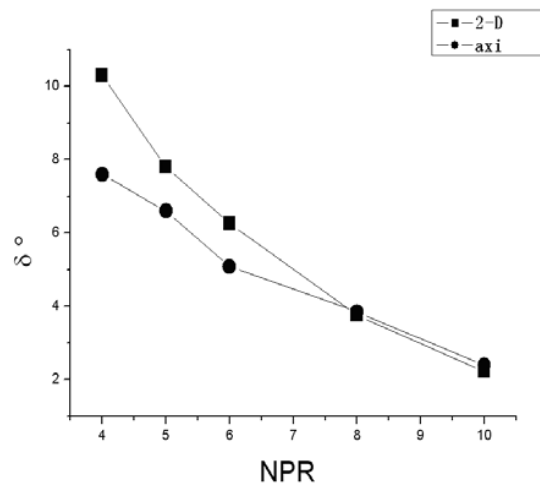


Fig. 10 The vector angle comparison with different NPR (  $\omega=4\%$  )

Fig.11 shows the thrust coefficient comparison of two nozzles for  $\omega=4\%$ . Generally, the thrust coefficient of the 2-D nozzle was higher than the axisymmetric nozzle's. For the 2-D nozzle, the highest thrust coefficient arisen at the NPR=6. For the axisymmetric nozzle, the thrust coefficient increased with the NPR increasing. However, the thrust coefficient of the axisymmetric nozzle was higher than that of the 2-D nozzle at the NPR=10.

Fig.13 shows the vector angle comparison of two nozzles under different NPR for the  $\omega=6\%$ . Likewise, the vector angle of 2-D nozzle was higher than that of the axisymmetric nozzle at the same NPR, and the highest vector angle was  $14^\circ$ . Differently, the vector angle difference was larger than that as  $\omega=4\%$ , as the recirculation area showed in Fig.14(b) was larger than that in Fig.14(a). The largest difference was  $5.17^\circ$  at the NPR=4.

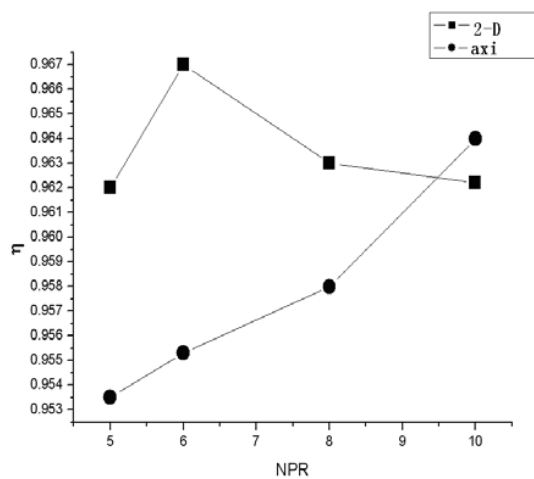


Fig. 11 The thrust coefficient comparison with different NPR ( $\omega=4\%$ )

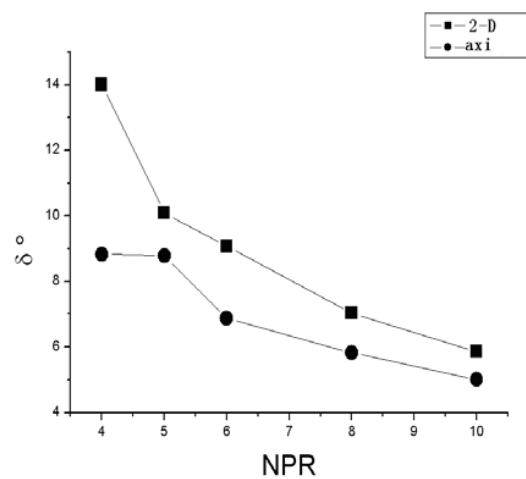
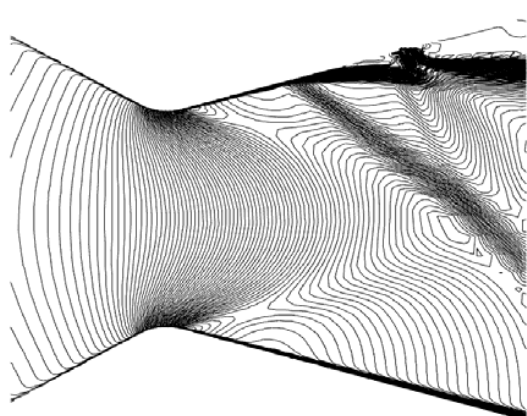
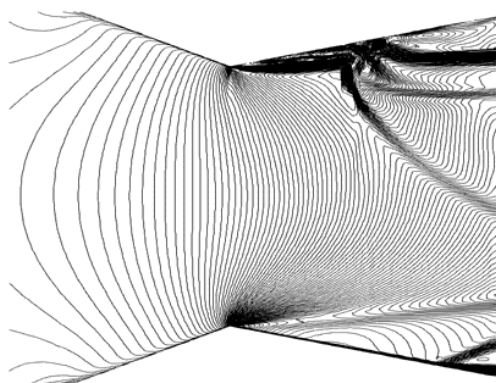


Fig. 13 The vector angle comparison with different NPR ( $\omega=6\%$ )

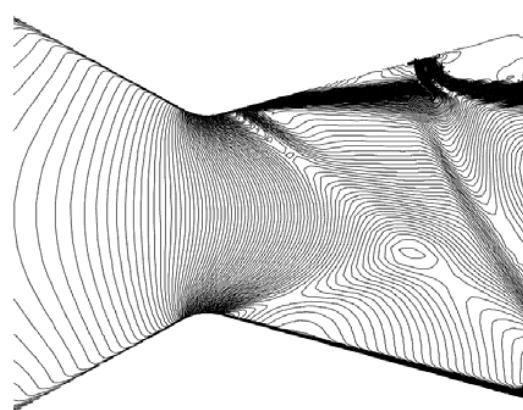


(a). Symmetry plane of 2-D nozzle

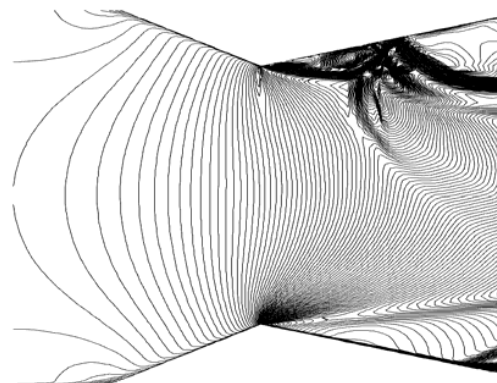


(b). Symmetry plane of axisymmetric nozzle

Fig. 12 The mach contours of two nozzles symmetry plane (NPR=4 $\omega=4\%$ )



(a). Symmetry plane of 2-D nozzle



(b). Symmetry plane of axisymmetric nozzle

Fig. 14 The mach contours of two nozzles symmetry plane (NPR=4 $\omega=6\%$ )



Fig.15 shows the vector angle comparison of two nozzles under different NPR for the  $\omega = 8\%$ . The whole trend was similar to that of  $\omega = 4\%, 6\%$ . The obvious difference was that with the higher secondary weight flow the vector angle difference was larger than the conditions above, especially under the lower NPR (NPR=4), the largest difference was  $7.08^\circ$ .

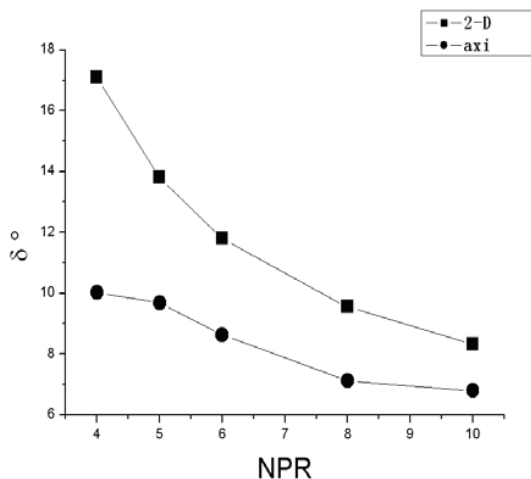


Fig. 15 The vector angle comparison with different NPR ( $\omega = 8\%$ )

Fig.16 shows the thrust coefficient comparison of two nozzles for  $\omega = 8\%$ . Similarly, the thrust coefficient of the 2-D nozzle was higher commonly. Under the lower NPR, the thrust coefficient between two nozzles differed much but less under the higher NPR.

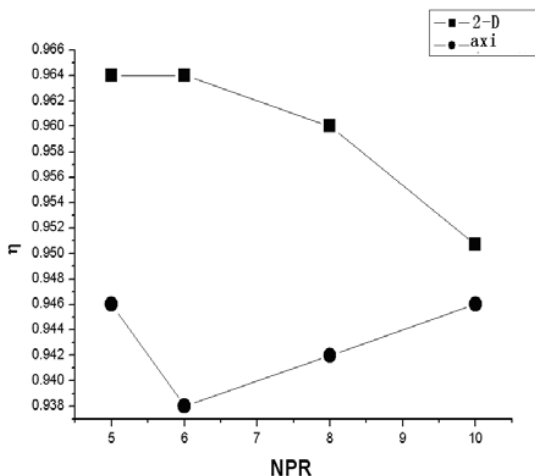
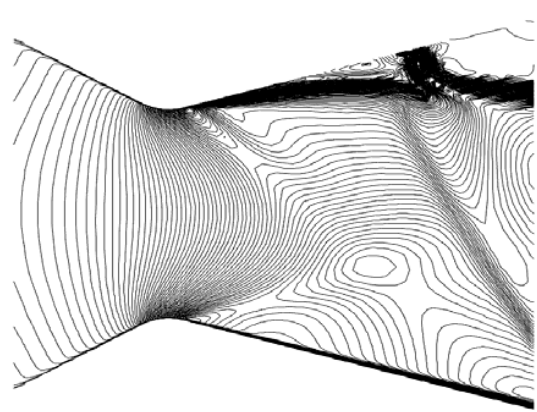
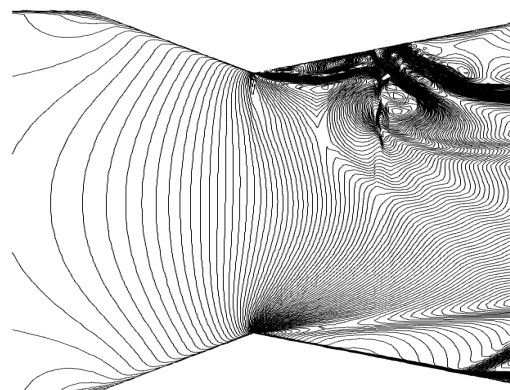


Fig. 16 The thrust coefficient comparison with different NPR ( $\omega = 8\%$ )



(a). symmetry plane of 2-D nozzle



(b). symmetry plane of axisymmetric nozzle

Fig. 17 The mach contours of two nozzles symmetry plane (NPR=4,  $\omega = 8\%$ )

#### IV. CONCLUSIONS

A computational study was completed on the two typical fluidic injection nozzles to document the effect of the external free stream flow on fluidic thrust vectoring effectiveness, the results indicated:

1. The thrust vector angles of two nozzles both increased with the increasing secondary flow but decreased with the nozzle pressure ratio (NPR) increasing.
2. At the same secondary flow and NPR, the thrust vector angles of 2-D nozzle was higher than the axisymmetric nozzle's.
3. With the higher NPR and less secondary weight flow, there was not much difference in angular dimension between two nozzles.
4. With the lower NPR and more secondary weight flow, the much higher thrust vector angle was caused by 2-D fluidic nozzle, and the highest vector angle was  $17.1^\circ$ .
5. At the most aerodynamic conditions, the thrust coefficient of the 2-D nozzle was higher than that of the axisymmetric nozzle. The highest the thrust coefficient was 0.964 at NPR=10.

$\omega=4\%$ .

#### APPENDIX

2-D 2-Demensional

NPR Nozzle pressure ratio

T Temperature, K

$\omega$  Secondary weight flow ratio

$\delta$  Thrust vector angle, deg

$\eta$  Thrust coefficient

#### REFERENCES

- [1] Wing D J. Static investigation of two fluidic. Thrust-vectoring concepts on a 2DCD nozzle [R]. N A S A-TM-4574, December, 1994
- [2] Wing David J, Giuliano V J. Fluidic Thrust Vectoring of an Axisymmetric Exhaust Nozzle at Static Conditions. ASMEFEDSM97-3228, 1997.
- [3] Jeffrey D. Flamm. Experimental Study of a Nozzle Using Fluidic Counterflow for Thrust Vectoring. AIAA98-3255, 1998
- [4] Deere K A. Summary of Fluidic Thrust Vectoring Research Conducted at NASA Langley Research Center. AIAA2003 - 3800 , 2003
- [5] Deere K A. Computational Investigation of the Aerodynamic Effects on Fluidic Thrust Vectoring. AIAA2000-3598 , 2000.
- [6] Deere K A, Waithe Kenrick A. Experimental and Computational Investigation of Multiple Injection Ports in a Convergent-Divergent Nozzle for Fluidic Thrust Vectoring. AIAA 2003-3802, 2003.